Synthesis, Properties, and Crystal Structures of Benzene-1,2-dithiolato Complexes of Thallium(I) and -(III)

Boris E. Bosch,[†] **Martin Eisenhawer,**[†] **Berthold Kersting,**[‡] **Kristin Kirschbaum,**[†] **Bernt Krebs,**[‡] **and Dean M. Giolando***[,†]

Department of Chemistry, University of Toledo, Toledo, Ohio 43606, and Anorganisch-Chemisches Institut, Universität Münster, 48149 Münster, Germany

Received November 2, 1995[⊗]

The syntheses, molecular structures and properties of homoleptic 1,2-$S_2C_6H_4$ complexes of thallium(I) and thallium(III) with four-coordinated metal centers are described. Anaerobic treatment of TlCl, $TlNO_3$, or Tl_2CO_3 with solutions of sodium methanolate and 1,2-$(HS)_2C_6H_4$ in methanol gave after metathesis with $[NEt_4]Br$ yellow solutions of $[NEt_4]_2[\{Tl(1,2\text{-}(\mu\text{-}S)_2C_6H_4)\}_2]$ ($[NEt_4]_2$**1**). Yellow single crystals were obtained from saturated acetone solutions at −10 °C and the crystal data for $[NEt_4]_2$**1** are monoclinic, $P2_1/c$, with $Z = 2$, $a = 7.440(1)$ Å, $b = 16.373(3)$ Å, $c = 13.201(2)$ Å, and $\beta = 97.08(1)°$. Complex $\mathbf{1}^{2-}$, the first structurally characterized homoleptic ionic thiolate complex of thallium(I), contains rectangular bipyramidal $[TlS_4Tl]$ cages with the four sulfur atoms defining the equatorial plane and the two thallium atoms in axial positions. The $S_2C_6H_4$ fragments are almost coplanar with the S_4 plane. In the crystal lattice, nearly linear Tl···Tl chains align along the *a*-axis (offset ca. 3.0°) with the ligand planes parallel to the *bc*-plane. Within and between dimers short Tl···Tl distances are observed (Tl···Tl′ within a dimeric unit, 3.5116(4) Å; Tl···Tl between dimeric units, 3.9371(3) Å) with the distance between dimeric units being the shortest contact between anions—Tl···S distances between dimeric units are longer than 5.8 Å. Aerobic treatment of TlCl, $TlNO_3$, or Tl_2CO_3 with solutions of sodium methanolate and 1,2-$(HS)_2C_6H_4$ in methanol and metathesis with $[NEt_4]Br$ led to $[NEt_4][Tl(1,2\text{-}S_2C_6H_4)_2]$ ($[NEt_4]$**2**). Yellow single crystals were obtained from saturated acetone solutions at 0 °C and the crystal data for $[NEt_4]$**2** are orthorhombic, *Pnn*2, with $Z = 2$, $a = 11.449(2)$ Å, $b = 10.060(2)$ Å, $c = 9.950(2)$ Å. Complex $\mathbf{2}^-$ is the first homoleptic four-coordinate thiolate of thallium(III) and contains the unusually short Tl−S distance of 2.469(4) Å. In solution, ion pairing results in chemical and magnetic inequivalence of the $S_2C_6H_4$ ligands. Although both preparations employ the reaction of thallium(I) salts with 1,2-$(NaS)_2C_6H_4$ in a 1:2 stoichiometry, complex $\mathbf{1}^{2-}$ is probably not an intermediate to the formation of $\mathbf{2}^-$. Exposing anaerobically prepared solutions of $\mathbf{1}^{2-}$ to air results in a series of color changes in the solution over a 20 min period; however, $\mathbf{2}^-$ could not be observed by NMR spectroscopy.

Introduction

Thiolate complexes of thallium have been known for many years and have received increased attention in the last years. During the past 40 years thiolate complexes of thallium have found applications ranging from analytical reagents[1] to model systems to study the environmental and toxicological impact of heavy metal biomethylation,[2] molecular precursors to solid state compounds of technological interest,[3] and, in the case of thallium(I), systems to explore the stereochemical activity of the s^2 lone pair of electrons.[4] While several classes of thallium(I) complexes have been identified, complexes of thallium(III) are not as diverse due to the oxidizing character of thallium(III).[5]

Structures containing thallium(I) are usually strongly influenced by the stereochemical demands of the lone pair of electrons, resulting in potentially reactive open coordination sites at the metal atom. Further interest is prompted by the presence of short Tl···Tl distances imposed by the geometrical constraints of the ligands or by Tl−Tl bonding interactions. Until recently, structural information on homoleptic thiolate complexes of thallium(I) were dominated by 1,1-S_2CNR_2 (where R = Me, Et, *n*-Pr, *i*-Pr, *n*-Bu, and *i*-Bu)[6,7] or 1,1-S_2PEt_2 derivatives.[8] The dimeric $[Tl(1,1\text{-}S_2CNR_2)]_2$ complexes contain bipyramidal TlS_4Tl cages loosely associated in polymeric structures with an alignment of Tl···Tl vectors with one of the crystallographic axes. The structure of $[Tl(1,1\text{-}S_2PEt_2)]$ is described as built-up of monomeric units, but resembles the $[Tl(1,1\text{-}S_2CNR_2)]_2$ complexes when the long intermolecular Tl···S distances are considered. Recent spectroscopic and structural results for a series of homoleptic thiolates of thallium(I), of the general formula TlSR (R = alkyl or aryl), reveal an interesting structural diversity as well as some indications of weak Tl···Tl interactions. The crystal structure of TlSPh consists of the clusters $[Tl_7(SPh)_6]^+$ and $[Tl_5(SPh)_6]^-$ linked by thiolate bridges, while TlS-*t*-Bu is comprised of discrete $[Tl_8(S\text{-}t\text{-}Bu)_8]$ molecules.[9] For

---

[†] University of Toledo.

[‡] Universität Münster.

[⊗] Abstract published in *Advance ACS Abstracts*, September 15, 1996.

(1) (a) Clark, R. E. D *Analyst*, **1957**, *82*, 177. (b) Spanyer, J. W.; Phillips, J. P. *Anal. Chem.* **1956**, *28*, 253.

(2) (a) Garcia-Tasende, M. S.; Suárez, M. I.; Sánchez, A.; Casas, J. S.; Sordo, J.; Castellano, E. E.; Mascarenhas, Y. P. *Inorg. Chem.* **1987**, *26*, 3818. (b) Castaño, M. V.; Macias, A.; Castiñeiras, A.; González, A. S.; Martínez, E. G.; Casas, J. S.; Sordo, J.; Hiller, W.; Castellano, E. E. *J. Chem. Soc., Dalton Trans.* **1990**, 1001.

(3) Krebs, B.; Brömmelhaus, A.; Kersting, B.; Nienhaus, M. *Eur. J. Solid State Inorg. Chem.* **1992**, *29*, 167.

(4) Dhingra, S. S.; Kanatzidis, M. G. *Inorg. Chem.* **1993**, *32*, 2298.

(5) Tuck, D. In *Comprehensive Coordination Chemistry*; Wilkinson, G., Gillard, R. D., McCleverty, J. A., Eds.; Pergamon Press: Oxford, England, 1987; Vol. 3, Chapter 25.

(6) (a) Nilson, L.; Hesse, R. *Acta Chem. Scand.* **1969**, *23*, 1951. (b) Jennische, P.; Olin, Å.; Hesse, R. *Acta Chem. Scand.* **1972**, *26*, 2799. (c) Jennische, P. ; Hesse, R. *Acta Chem. Scand.* **1973**, *27*, 3531. (d) Anacker-Eickhoff, H.; Jennische, P.; Hesse, R. *Acta Chem. Scand.* **1975**, *A29*, 51. (e) Pritzkow, H; Jennische, P. *Acta Chem. Scand.* **1975**, *A29*, 60. (f) Elfwing, E.; Anacker-Eickhoff, H.; Jennische, P.; Hesse, R. *Acta Chem. Scand.* **1976**, *A30*, 335.

(7) Coucouvanis, D. *Prog. Inorg. Chem.* **1979**, *26*, 301.

(8) Esperås, S.; Husebye, S. *Acta Chem. Scand.* **1974**, *A28*, 1015.

S0020-1669(95)01411-X CCC: $12.00

TlS-*i*-Pr the solid state structure contains $[Tl_4(S\text{-}i\text{-}Pr)_5]^-$ cages that form a polymeric chain by way of additional thallium cations.[10] In addition to the formation of three-dimensional clusters, two-dimensional polymers consisting of linked 1,3-Tl_2S_2 rings have been described[9a,10,11] for $TlSCH_2Ph$, $TlSC_6H_{11}$, and $Tl\{2,4,6\text{-}SC_6H_2(CF_3)_3\}\cdot0.5$ dioxane. Bulky ligands provide a dimeric complex[12] in $[Tl(SSi\{O\text{-}t\text{-}Bu\}_3)]_2$, which also contains a 1,3-Tl_2S_2 ring. Interestingly, isoelectronic $TlSCH_2Ph$ and $Pb(SCH_2Ph)_2$ possess similar polymeric structures, while crystals of $Pb(SC_6H_{11})_2$ in contrast to $TlSC_6H_{11}$ contain a two-dimensional network of sulfur linked hexameric $Pb_6(SC_6H_{11})_{12}$-units.[13] Surprisingly, synthetic and crystallographic studies of 1,2-dithiolate complexes of thallium(I) are very limited.[14]

To our knowledge the only structurally characterized examples of homoleptic thiolate complexes of thallium(III) are the complexes[15] $[Tl(1,1\text{-}S_2CNR_2)_3]$, where R = Me or Et. While the chemistry of 1,2-dithiolate complexes of thallium(III) is slightly more mature than for thallium(I), the only structural result is the heteroleptic complex[16] $[N\text{-}n\text{-}Bu_4]_2[Tl\{1,2\text{-}S_2C_2(CN)_2\}_2Br]$. Homoleptic $[Tl(dithiolene)_2]^-$ complexes, where dithiolene denotes 1,2-$S_2C_2H_2$, 4,5-$S_2C_6H_2(CH_3)_2$, or 1,2-$S_2C_2(CN)_2$, have been prepared and characterized by NMR and electronic spectroscopies and conductivity measurements.[17] Thiolate complexes with six-coordinate main group metal centers are not common; however, a few $[Tl(dithiolene)_3]^{3-}$ complexes, where dithiolene denotes 1,1-$S_2C_2N_2$, 1,2-$S_2C_2(CN)_2$, S_5C_3 (2-thioxo-1,3-dithiole-4,5-dithiolate, dmit), and S_5C_3 (3-thioxo-1,2-dithiole-4,5-dithiolate, dmt) were prepared and characterized.[17b,18] This scarcity of information on 1,2-dithiolate complexes prompted our investigation into the chemistry of 1,2-$S_2C_6H_4$ complexes of thallium. We report in this paper syntheses, structural characterizations and properties of two homoleptic four-coordinate thiolate complexes of thallium, $[NEt_4]_2[\{Tl(1,2\text{-}(\mu\text{-}S)_2C_6H_4)\}_2]$ ($[NEt_4]_2$**1**) and $[NEt_4][Tl(1,2\text{-}S_2C_6H_4)_2]$ ($[NEt_4]$**2**). Structurally, $\mathbf{1}^{2-}$ and $\mathbf{2}^{-}$ are very rare 1,2-dithiolate complexes of thallium. Additionally, the structural results for $\mathbf{1}^{2-}$ reveal short Tl···Tl interactions that are unsupported by bridging ligands.

Experimental Section

Chemicals and Instrumentation. All reagents were newly purchased from commercial sources and used without further purification except where noted. Sodium metal, $[NEt_4]Br$, $[N\text{-}n\text{-}Bu_4]I$, acetonitrile-$d_3$, acetone-$d_6$, dimethyl-$d_6$ sulfoxide, and chloroform-*d* were obtained from Aldrich Co. The thallium(I) salts TlCl, $TlNO_3$, and Tl_2CO_3 were purchased from Strem Chemicals. The compound 1,2-$(HS)_2C_6H_4$ was prepared by a literature method.[19] All solvents were procured from Fisher and distilled: diethyl ether and THF from Na−benzophenone; *N*,*N*-dimethylformamide, acetone, dichloromethane, and chloroform from P_2O_5; methanol and ethanol from Na; acetonitrile from CaH_2. *N*,*N*-Dimethylformamide was deoxygenated by vacuum distillation. $[N\text{-}n\text{-}Bu_4][PF_6]$ was recrystallized from hot ethanol. Proton, ^{13}C, $^{13}C\{APT\}$ and COSY NMR spectra were obtained using a Varian VXR-400 FT NMR spectrometer. UV−vis spectra were recorded on a Varian Cary 5 UV/vis/near-IR spectrophotometer. Cyclic voltammograms were obtained on a BAS CV 1B cyclic voltammograph. Elemental analyses were carried out with a Perkin-Elmer CHN elemental analyzer, Model 2400. Vapor pressure osmometry was performed by Galbraith Laboratories. All experimental work was performed under an inert atmosphere using deoxygenated solvents if not otherwise mentioned.

Synthesis of $[NEt_4]_2[\{Tl(1,2\text{-}(\mu\text{-}S)_2C_6H_4)\}_2]$ ($[NEt_4]_2$1). In a typical experiment, 1,2-$(HS)_2C_6H_4$ (0.142 g, 1.0 mmol) in methanol (50 mL) was added dropwise to a solution of sodium methanolate in methanol (22.0 mL, 2.2 mmol, 0.10 mol L^{-1}) and stirred for 1 h. Afterward, a suspension of $TlNO_3$ (0.133 g, 0.50 mmol) in a solution of sodium methanolate in methanol (30 mL, 3.0 mmol, 0.10 mol L^{-1}) was added dropwise. At this point the reaction flask was covered with aluminum foil. The solution was stirred for 18 h and then treated with $[NEt_4]Br$ (0.210 g, 1.0 mmol) in methanol (10 mL). The resultant yellow solution was stirred for 48 h. Volatile materials were removed in vacuo and the yellow residue was extracted with warm acetone (40 mL × 3, 50 °C, 2 h vigorous stirring) and filtered. The combined filtrates were stored at −10 °C for 72 h whereupon yellow crystals precipitated (0.071 g, 0.075 mmol, 30% yield based on thallium) which do not redissolve readily. Anal. Calcd for $C_{28}H_{48}N_2S_4Tl_2$: C, 35.41; H, 5.09; N, 2.95. Found: C, 35.72; H, 5.21; N, 2.92. ^1H NMR (acetonitrile-d_3, 21 °C): δ 7.36 (m, 1H, $S_2C_6H_4$), 6.46 (m, 1H, $S_2C_6H_4$), 3.11 (q, $^3J_{C-H}$ = 7.3 Hz, 4H, NCH_2CH_3), 1.17 (t, $^3J_{C-H}$ = 7.3 Hz, 6H, NCH_2CH_3). ^{13}C NMR (acetonitrile-d_3, 21 °C): insufficient solubility.

Synthesis of $[NEt_4][Tl(1,2\text{-}S_2C_6H_4)_2]$ ($[NEt_4]$2). In a typical experiment conducted in air, 1,2-$(HS)_2C_6H_4$ (0.500 g, 3.52 mmol) in methanol (50 mL) was added dropwise to a solution of sodium methanolate in methanol (4.0 mL, 10 mmol, 2.5 mol L^{-1}) and stirred for 1 h. Afterward, a suspension of $TlNO_3$ (0.480 g, 1.80 mmol) in methanol (30 mL) was added dropwise. The reaction mixture turns yellow, and a small quantity of an orange-red precipitate forms that typically dissolves within 12 h. The solution was stirred for 18 h and then treated with $[NEt_4]Br$ (0.420 g, 2.0 mmol) in methanol (10 mL). The resultant yellow solution was stirred for 48 h. Volatile materials were removed in vacuo, and the residue was extracted with boiling acetone (40 mL x 3) and filtered. The combined filtrates were stored at −10 °C for 72 h whereupon yellow crystals precipitated (1.05 g, 1.71 mmol, 95% yield based on thallium). Anal. Calcd for $C_{20}H_{28}NS_4Tl$: C, 39.06; H, 4.59; N, 2.28. Found: C, 38.81; H, 4.60; N, 2.35. ^1H NMR (acetonitrile-d_3, 21 °C): δ 7.55 (m, 1H, $S_2C_6H_4$), 7.51 (m, 1H, $S_2C_6H_4$), 6.74 (m, 2H, $S_2C_6H_4$), 3.13 (q, $^3J_{C-H}$ = 7.3 Hz, 4H, NCH_2CH_3), 1.18 (t, $^3J_{C-H}$ = 7.3 Hz, 6H, NCH_2CH_3). ^1H NMR (acetone-d_6, 21 °C): δ 7.52 (m, 1H, $S_2C_6H_4$), 7.48 (m, 1H, $S_2C_6H_4$), 6.67 (m, 2H, $S_2C_6H_4$), 3.45 (q, $^3J_{C-H}$ = 7.6 Hz, 4H, NCH_2CH_3), 1.36 (t, $^3J_{C-H}$ = 7.6 Hz, 6H, NCH_2CH_3).

Synthesis of $[N\text{-}n\text{-}Bu_4][Tl(1,2\text{-}S_2C_6H_4)_2]$ ($[N\text{-}n\text{-}Bu_4]$2). The synthetic procedure for $[N\text{-}n\text{-}Bu_4]$**2** was identical to that described for $[NEt_4]$**1** except in the metathesis step $[N\text{-}n\text{-}Bu_4]I$ (0.730 g, 1.97 mmol) was used. The product was recrystallized by adding 1 mL of methanol to concentrated acetone solutions that on cooling to −20 °C yielded yellow crystals of $[N\text{-}n\text{-}Bu_4]$**2** (1.20 g, 1.58 mmol, 88% based on thallium). Anal. Calcd for $C_{28}H_{44}NS_4Tl$: C, 46.24; H, 6.10; N, 1.93. Found: C, 46.41; H, 5.98; N, 1.96. ^1H NMR (acetonitrile-d_3, 21 °C): δ 7.53 (br s, 2H, $S_2C_6H_4$), 6.74 (m, 2H, $S_2C_6H_4$), 3.04 (m, 4H, $N(CH_2)_3CH_3$), 1.57 (m, 4H, $N(CH_2)_3CH_3$), 1.32 (m, 4H, $N(CH_2)_3CH_3$), 0.95 (m, 6H, $N(CH_2)_3CH_3$). ^1H NMR (acetone-d_6, 21 °C): δ 7.54 (m, 1H, $S_2C_6H_4$), 7.50 (m, 1H, $S_2C_6H_4$), 6.69 (m, 2H, $S_2C_6H_4$), 3.39 (m, 4H, $N(CH_2)_3CH_3$), 1.78 (m, 4H, $N(CH_2)_3CH_3$), 1.41 (m, 4H, $N(CH_2)_3CH_3$), 0.96 (m, 6H, $N(CH_2)_3CH_3$). ^1H NMR (chloroform-*d*, 21 °C): δ 7.61

---

(9) (a) Krebs, B.; Brömmelhaus, A. *Z. Anorg. Allg. Chem.* **1991**, *595*, 167. (b) Krebs, B.; Brömmelhaus, A. *Angew. Chem., Int. Ed. Engl.* **1989**, *28*, 1682.

(10) Brömmelhaus, A.; Pinkerton, A. A.; Krebs, B. Annual Meeting of the American Crystallographic Association, Toledo, OH, 1991; Abstract p.123.

(11) Labahn, D.; Pohl, E.; Herbst-Irmer, R.; Stalke, D.; Roesky, H. W.; Sheldrick, G. M. *Chem. Ber.* **1991**, *124*, 1127.

(12) Wojnowski, W.; Peters, K.; Peters, E.-M.; Schnering, H. G. v. *Z. Anorg. Allg. Chem.* **1985**, *531*, 147.

(13) Krebs, B.; Ahlers, F. P.; Bonmann, S.; Brömmelhaus, A.; Greiwing, H.; Kersting, B.; Kirschbaum, K.; Lindner, T.; Nienhaus, M; Taubken, N. *Unkonventionelle Wechselwirkungen in der Chemie Metallischer Elemente*; Krebs, B., Ed., VCH Verlagsgesellschaft: Weinheim, Germany 1991; p 139.

(14) Dräger, M.; Gattow, G. *Z. Anorg. Allg. Chem.* **1972**, *387*, 300.

(15) (a) Abrahamson, H.; Heiman, J. R.; Pignolet, L. H. *Inorg. Chem.* **1975**, *14*, 2070. (b) Kepert, D. L.; Raston, C. L.; Roberts, N. K.; White, A. H. *Aust. J. Chem.* **1978**, *31*, 1927.

(16) Day, R. O.; Holmes, R. R. *Inorg. Chem.* **1982**, *21*, 2379.

(17) (a) Hoyer, E.; Dietzsch, W.; Müller, H.; Zschunke, A.; Schroth, W. *Inorg. Nucl. Chem. Lett.* **1967**, *3*, 457. (b) Fields, R. O.; Waters, J. H.; Bergendahl, T. J. *Inorg. Chem.* **1971**, *10*, 2808. (c) Hunter, G.; Williams, B. C. *J. Chem. Soc. A* **1971**, 2554.

(18) (a) Cotton, F. A.; McCleverty, J. A. *Inorg. Chem.* **1967**, *6*, 229. (b) Olk, R.-M.; Dietzsch, W.; Kirmse, R.; Stach, J.; Hoyer, E.; Golic, L. *Inorg. Chim. Acta* **1987**, *128*, 251.

(19) Giolando, D. M.; Kirschbaum, K. *J. Synth. Org. Chem.* **1992**, *5*, 451.

(m, 1H, $S_2C_6H_4$), 7.57 (m, 1H, $S_2C_6H_4$), 6.75 (m, 2H, $S_2C_6H_4$), 2.93 (m, 4H, $N(CH_2)_3CH_3$), 1.41 (m, 4H, $N(CH_2)_3CH_3$), 1.35 (m, 4H, $N(CH_2)_3CH_3$), 0.95 (m, 6H, $N(CH_2)_3CH_3$). ^1H NMR (dimethyl-d_6 sulfoxide, 21 °C): δ 7.49 (m, 1H, $S_2C_6H_4$), 7.47 (m, 1H, $S_2C_6H_4$), 6.74 (m, 2H, $S_2C_6H_4$), 3.13 (m, 4H, $N(CH_2)_3CH_3$), 1.54 (m, 4H, $N(CH_2)_3CH_3$), 1.30 (m, 4H, $N(CH_2)_3CH_3$), 0.92 (m, 6H, $N(CH_2)_3CH_3$). ^{13}C NMR (acetonitrile-d_3, 20 °C): δ 141.5 ($S_2C_6H_4$), 133 (v br, $S_2C_6H_4$), 130 (v br, $S_2C_6H_4$), 123 (br, $S_2C_6H_4$), 59.3 ($N(CH_2)_3CH_3$), 24.3 ($N(CH_2)_3CH_3$), 20.3 ($N(CH_2)_3CH_3$), 13.8 ($N(CH_2)_3CH_3$). ^{13}C NMR (acetone-d_6, 20 °C): δ 142.0 ($S_2C_6H_4$), 134.8 ($S_2C_6H_4$), 128.3 ($S_2C_6H_4$), 123.0 ($S_2C_6H_4$), 122.5 ($S_2C_6H_4$), 59.3 ($N(CH_2)_3CH_3$), 24.3 ($N(CH_2)_3CH_3$), 20.3 ($N(CH_2)_3CH_3$), 13.8 ($N(CH_2)_3CH_3$).

Collection and Reduction of X-ray Data, $[NEt_4]_2$1 and $[NEt_4]$2. Single crystals selected for data collection were mounted with a trace of silicon grease on a glass fiber. X-ray diffraction data were collected with an Enraf-Nonius CAD-4 diffractometer (graphite monochromated, λ(Mo Kα) = 0.710 73 Å) in the $\omega-2\theta$ mode. Data were collected at 177(1) K for $[NEt_4]_2$**1** (203(1) K for $[NEt_4]$**2**) to a maximum 2θ of 52°. The unit cell dimensions and their standard deviations were derived from a least-squares fit of the setting angles of 25 centered reflections in the range of $10° < \theta < 15°$. The intensities of three standard reflections were measured every 50 min. Anisotropic decay corrections were applied with correction factors on I ranging from 0.960 to 1.034 (0.977 to 1.027). The raw intensity data were corrected for Lorentz and polarization effects. A semiempirical absorption correction ($\psi-$scan) was applied to the data set of $[NEt_4]_2$**1**. An empirical absorption correction was applied to the data set of $[NEt_4]$**2**. Intensities of equivalent reflections were averaged; the agreement factor based on I is 2.9% (3.5%). A total of 3513 (1813) reflections were measured, of which 3259 (1485) were unique and 2157 (882) reflections with $F_o^2 > 3.0\sigma(F_o^2)$ were used in the calculations.

Solution and Refinement of $[NEt_4]_2$1 and $[NEt_4]$2. All calculations were performed on a VAX 3100 computer using MolEN.[20] $[NEt_4]_2$**1**: The observed systematic absences were consistent with the monoclinic space group $P2_1/c$. A secondary extinction coefficient refinement was applied. $[NEt_4]$**2**: The observed systematic absences were consistent with the orthorhombic space groups $Pnn2$ and $Pnnm$. The distribution of the normalized structure factors indicated the noncentrosymmetric space group. The structure solution and refinement confirmed this choice.

Starting models for both structures were provided by the heavy atom method. These starting models were further developed to final structure models with anisotropic thermal parameters for the non-hydrogen atoms (with the exception of the disordered methylene carbon atoms in the cation of $[NEt_4]$**2**, which were refined with isotropic thermal parameters). Hydrogen atoms were calculated on idealized positions (C−H bond of 0.95 Å) with $U_{iso} = 1.3\ U$(bonding atom) and included in the refinement as riding atoms. The final full-matrix least-squares refinement cycles included 164(116) variable parameters and converged with $R = \sum||F_o| - |F_c||/\sum|F_o| = 3.0(3.1)\%$ and $R_w = [\sum w(|F_o| - |F_c|)^2/\sum w|F_o|^2]^{1/2} = 4.9(3.3)\%$. The function minimized during refinement was $\sum w(|F_o| - |F_c|)^2$, $w = 4F_o^2/\sigma^2(F_o)^2$. Atomic scattering factors for spherical neutral free (non H-atoms) or bonded (H) atoms as well as anomalous scattering contributions were taken from standard literature.[21] Crystal data are given in Table 1, and selected distances and angles are given in Tables 2 and 3.

Results and Discussions

Synthesis and Characterization. In addition to the methods of Tuck,[22] which employ thallium metal, thiolate complexes of thallium are usually prepared via a salt elimination reaction between sources of a cationic thallium and anionic thiolates.

Table 1. Details Relevant to the Data Collection and Structure Refinements

	$[NEt_4]_2$-$[\{Tl(1,2\text{-}(\mu\text{-}S)_2C_6H_4)\}_2]$	$[NEt_4]$-$[Tl(1,2\text{-}S_2C_6H_4)_2]$
formula	$C_{28}H_{48}Tl_2N_2S_4$	$C_{20}H_{28}TlNS_4$
fw	949.70	615.08
color and habit	yellow, orthogonal	yellow, chunky
cryst size, mm^3	0.15 × 0.20 × 0.30	0.20 × 0.20 × 0.10
cryst system	monoclinic	orthorhombic
space group	$P2_1/c$	$Pnn2$
a, Å	7.440(1)	11.449(2)
b, Å	16.373(3)	10.060(2)
c, Å	13.201(2)	9.950(2)
β, deg	97.08(1)	
vol, Å^3	1597(1)	1146(1)
Z	2	2
D_{calcd}, g cm^{-3}	1.98	1.78
μ, cm^{-1}	104.6	74.8
no. of obsd reflns	3513	1813
no. of unique reflns,[a]	2157	882
R,[b] R_w[c]	0.030, 0.049	0.031, 0.033
goodness of fit[d]	2.16	2.24
temp, K	177(1)	203(1)

[a] $I > 3.0\sigma(I)$. [b] $R = \sum||F_o| - |F_c||/\sum|F_o|$. [c] $R_w = [\sum w(|F_o| - |F_c|)^2/\sum w|F_o|^2]^{1/2}$. [d] GOF $= [\sum w(|F_o| - |F_c|)^2/(N_o - N_v)]^{1/2}$.

Table 2. Selected Distances (Å) and Angles (deg) for $[NEt_4]_2[\{Tl(1,2\text{-}(\mu\text{-}S)_2C_6H_4)\}_2]$[a]

Tl−Tl′	3.5116(4)	Tl−Tl*	3.937(1)
Tl−S1	2.876(2)	S1−S2	3.360(3)
Tl−S2	2.858(2)	S1−S2′	3.669(3)
Tl−S1′	3.074(2)	S1−S1′	4.808(3)
Tl−S2′	3.346(2)	S2−S2′	5.138(3)
S1−C1	1.775(8)	S2−C2	1.768(7)
S1−T1−S2	71.76(5)	T1−S2′−C2′	96.9(2)
S1−T1−S1′	107.75(5)	T1−S1′−T1′	72.25(4)
S1−T1−S2′	71.81(5)	T1−S2−T1′	68.42(4)
S2−T1−S1′	76.33	T1−S1−Cl	102.4(2)
S2−T1−S2′	111.58(5)	T1−S2−C2	102.3(3)
S1′−T1−S2′	62.95(5)	S1−S2−S1′	86.18(6)
T1−S1′−C1′	102.5(3)	S2−S1−S2′	93.82(6)

[a] Symmetry operations: (′), $1 - x, -y, -z$; (*), $-x, -y, -z$.

Table 3. Selected Bond Distances (Å) and Angles (deg) for $[NEt_4][Tl(1,2\text{-}S_2C_6H_4)_2]$[a]

Tl−S1	2.469(4)	S1−C1	1.76(1)
Tl−S2	2.469(4)	S2−C2	1.77(1)
S1−Tl−S2	89.6(1)	S2−Tl−S2′	116.1(1)
S1−Tl−S1′	117.5(1)	Tl−S1−C1	98.6(4)
S2−Tl−S1′	123.7(1)	Tl−S2−C2	98.9(4)

[a] Symmetry operation (′): $-x, 1 - y, z$.

Either TlCl or TlX_3, where X = Cl or O_2CCH_3, can be employed[17b,c] in the preparation $[Tl(1,2\text{-dithiolate})_2]^-$. For the thallium(I) reagents air oxidation generates a thallium(III) product.[17] To our knowledge 1,2-dithiolate complexes of thallium(I) have not been described, but they may be an intermediate in these reactions. Hunter[17c] describes the preparation of $[Tl\{1,2\text{-}S_2C_2(CN)_2\}_y]^{z-}$, where $(y, z) = (2, 1)$ or $(3, 3)$, from $TlCl_3$; however, Waters[17b] reports the presence of halide affords either $[Tl\{1,2\text{-}S_2C_2(CN)_2\}_3]^{3-}$ or $[TlX\{1,2\text{-}S_2C_2(CN)_2\}_2]^{2-}$, where X is Cl or Br. Interestingly, $[Tl(1,2\text{-dithiolate})_3]^{3-}$ complexes have not been prepared for either the $1,2\text{-}S_2C_6H_4$ or $1,2\text{-}S_2C_2H_2$ derivatives.

Reaction of $TlNO_3$ with $1,2\text{-}(NaS)_2C_6H_4$ in a 1:2 stoichiometry produces either $Na_2[\{Tl(1,2\text{-}(\mu\text{-}S)_2C_6H_4)\}_2]$, under anaerobic conditions, or $Na[Tl(1,2\text{-}S_2C_6H_4)_2]$, under aerobic conditions (Scheme 1). The complex anions were isolated, after metathesis with $[NEt_4]$Br and acetone extraction, as yellow crystalline salts

---

(20) Fair C. K., *MolEN, An Interactive Intelligent System for Crystal Structure Analysis, User Manual*; Enraf-Nonius: Delft, The Netherlands, 1990.

(21) *International Tables for X - ray Crystallography*; Kynoch Press: Birmingham, England, 1974; Vol. IV.

(22) (a) Kumar, R.; Mabrouk, H. E.; Tuck, D. G. *J. Chem. Soc., Dalton Trans.* **1988**, 1045. (b) Green, J. H.; Kumar, R.; Seudeal, N.; Tuck, D. G. *Inorg. Chem.* **1989**, *28*, 123 and references therein.

Scheme 1

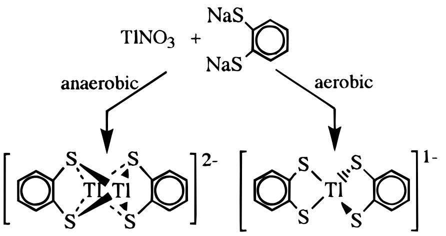

of $[NEt_4]_2[\{Tl(1,2\text{-}(\mu\text{-}S)_2C_6H_4)\}_2]$ ($[NEt_4]_2$**1**) and $[NEt_4][Tl(1,2\text{-}S_2C_6H_4)_2]$ ($[NEt_4]$**2**). To facilitate spectroscopic studies [N-*n*-Bu$_4$]$[Tl(1,2\text{-}S_2C_6H_4)_2]$ ([N-*n*-Bu$_4$]**2**) was also prepared due to its increased solubility. Apparently, the thallium source was unimportant to the outcome of these reactions since TlCl, $TlNO_3$, and Tl_2CO_3 provide the same final product in similar yields.

Synthetic procedures for the preparation of compounds of thallium(I) are often sensitive to exposure to air and light,[9] which proved to be the case for $[NEt_4]_2$**1**. Reactions unprotected from sources of light produce very low yields of product or intractable yellow oils. During efforts to optimize the synthesis of $[NEt_4]_2$**1** a reaction of $TlNO_3$ and $1,2\text{-}(NaS)_2C_6H_4$ in a 1:1 stoichiometry was examined and found to produce heterogeneous mixtures from which as yet unidentified feathery yellow crystallites are obtained. Optimal yields of $[NEt_4]_2$**1** (ca. 30% isolated yields) are achieved with the reaction of $TlNO_3$ and $1,2\text{-}(NaS)_2C_6H_4$ in a 1:2 stoichiometry. Once formed, crystalline $[NEt_4]_2$**1** is poorly soluble in acetonitrile, acetone, and *N,N*-dimethylformamide and insoluble in other common organic solvents. Solutions of $[NEt_4]_2$**1** are air-sensitive; on contact with small amounts of air, solutions undergo a series of color changes: yellow to orange to red to, finally, black. Solubility of $[NEt_4]_2$**1** in acetonitrile-d_3 is insufficient to obtain a ^{13}C NMR spectrum; however, the ^1H NMR spectrum is observable, which contains two multiplets interpreted as a AA′BB′ spin system at 7.36 and 6.46 ppm. This observed pattern agrees with the symmetric structure obtained by X-ray crystallography. Results of the cyclic voltammetric investigations of $[NEt_4]_2$**1**, using a three-electrode cell (Pt-disk working electrode, cycling between -1.9 and $+1.7$ V, negative and positive scans starting from 0.0 V), are interpreted as an irreversible reduction with a peak potential of ca. -0.85 V (vs Ag/AgCl, in *N,N*-dimethylformamide). The electrochemical process involves the conversion of thallium(I) to thallium metal, as evidenced by the production of thallium metal on the surface of the working electrode. Figure 1 contains a series of cyclic voltammograms obtained as potential is cycled between the limits of -0.3 and -1.3 V (vs Ag/AgCl). The incremental growth and narrowing of the reduction half-wave at ca. -0.85 V (vs Ag/AgCl) is characteristic of the growth of an adsorbed species onto the surface of the electrode.

Aerobic treatment of $TlNO_3$ with a solution of $1,2\text{-}(HS)_2C_6H_4$ in sodium methanolate/methanol initially produces a suspension containing an orange-red precipitate that dissolves completely within 12 h. Metathesis of the resultant yellow solutions with either $[NEt_4]Br$ or [N-*n*-Bu$_4$]I affords a yellow precipitate of $[NEt_4]$**2** (ca. 95% isolated yield) or [N-*n*-Bu$_4$]**2** (ca. 88% isolated yield). These tetraalkyl ammonium salts are soluble in acetonitrile, acetone, and *N,N*-dimethylformamide, modestly soluble in dichloromethane and chloroform, and insoluble in H_2O, methanol, diethyl ether, and tetrahydrofuran. Solid samples and solutions of $[NR_4]$**2** are air stable. Nuclear magnetic resonance spectra of **2**$^-$ are unexpectedly complicated and are discussed later. Results of the cyclic voltammetric investigations of $[NEt_4]$**2**, using a three-electrode cell (Pt-disk working electrode, cycling between -1.9 and $+1.7$ V, negative and positive scans starting from 0.0 V), are interpreted as an irreversible oxidation wave with a peak potential of ca. 0.63 V (vs Ag/AgCl, in *N,N*-dimethylformamide). In contrast, the electrochemical characterization of $[Tl(1,2\text{-}S_2C_2H_2)_2]^-$ was interpreted as a reversible reduction at a peak potential of -0.74 V and an irreversible oxidation at a peak potential of -0.28 V (vs SCE, 0.1 M $NaClO_4$, in dimethyl sulfoxide).[17a]

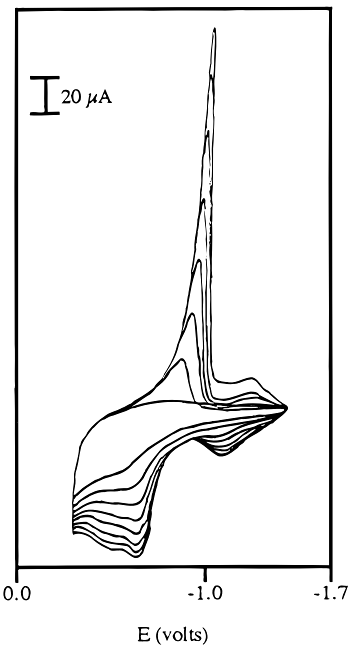

Figure 1. Cyclic voltammograms of $[NEt_4]_2[\{Tl(1,2\text{-}(\mu\text{-}S)_2C_6H_4)\}_2]$ obtained by cycling between the limits of -0.3 and -1.3 V (vs Ag/AgCl).

Crystal Structures. Structural analyses of $[NEt_4]_2$**1** and $[NEt_4]$**2** by X-ray crystallography reveal the presence of discrete anionic $1,2\text{-}S_2C_6H_4$ complexes of thallium and $[NEt_4]^+$ cations; the shortest interanionic Tl$-$S interactions are greater than 5.8 Å. Both anions, **1**$^{2-}$ and **2**$^-$, contain thallium atoms solely coordinated by four sulfur atoms of $1,2\text{-}S_2C_6H_4$-ligands. Bond distances within the $S_2C_6H_4$-ligands are very similar to those found in $[M(1,2\text{-}S_2C_6H_4)_3]^{z-}$, where (M, *z*) = (Ti, 2), (Zr, 2), (Ta, 2), and (Sb, 1) and are interpreted as indicating dithiolato, rather than dithioketonic, character.[23,24]

Recrystallization of $[NEt_4]_2$**1** from warm acetone provides pale yellow crystals suitable for X-ray crystallography. Figure 2 shows the molecular structure of the anion **1**$^{2-}$ along with the numbering scheme. The crystal structure of $[NEt_4]_2$**1** contains dimers of **1**$^{2-}$, which are centrosymmetric about an inversion center formed by two $[Tl(1,2\text{-}S_2C_6H_4)]^-$ monomeric units. The Tl_2S_4 core can be described as a distorted rectangular bipyramidal $[TlS_4Tl]$ cage with the four sulfur atoms defining the equatorial plane and the two thallium atoms the axial positions. Each thallium atom and the four sulfur atoms constitute a distorted rectangular pyramid with the thallium lone pair electrons in the apical vertex. Each of the sulfur atoms is three-coordinated and bridges the two thallium atoms with one short and one long Tl$-$S bond {2.867(average) and 3.210(average) Å}. Within a monomeric unit Tl$-$S distances {Tl$-$S1 2.876(2) Å and Tl$-$S2 2.858(2) Å} are short for thallium(I), and are comparable to other short Tl$-$S distances {$[Tl\{1,1\text{-}S_2CN(i\text{-}Pr)_2\}]_2$ 2.88(1) Å, $[\{TlSSi(O\text{-}t\text{-}Bu)_3\}_2]$ 2.880(2) Å,

---

(23) Wegener, J.; Kirschbaum, K.; Giolando, D. M. *J. Chem. Soc., Dalton Trans.* **1994**, 1213.

(24) (a) Könemann, M.; Stüer, W.; Kirschbaum, K.; Giolando, D. M. *Polyhedron* **1994**, *13*, 1415. (b) Cowie, M.; Bennett, M. J. *Inorg.Chem.* **1976**, *15*, 1595; (c) Martin, J. L.; Takats, J. *Inorg. Chem.* **1975**, *14*, 1358.

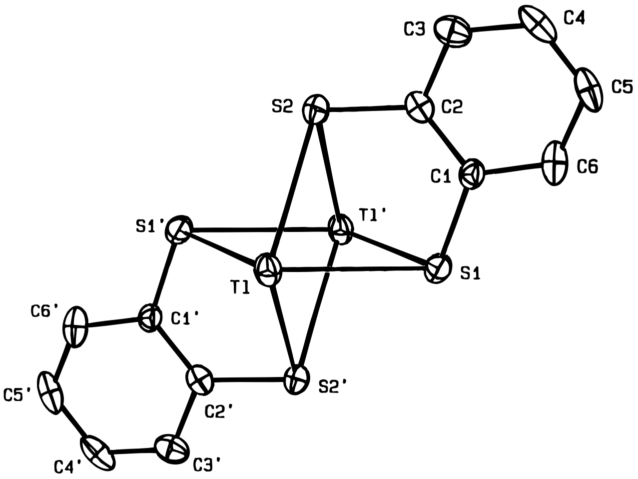

Figure 2. ORTEP plot and numbering scheme of the complex anion of $[NEt_4]_2[\{Tl(1,2\text{-}(\mu\text{-}S)_2C_6H_4)\}_2]$ with 50% probability ellipsoids.

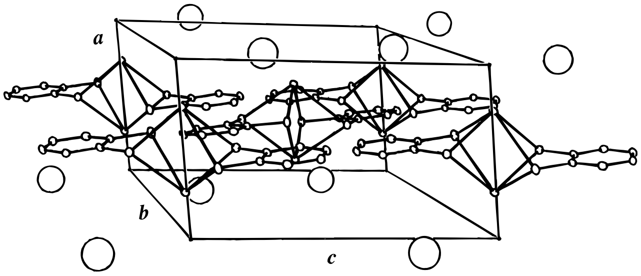

Figure 3. Unit cell view of $[NEt_4]_2[\{Tl(1,2\text{-}(\mu\text{-}S)_2C_6H_4)\}_2]$. The cation is represented by a sphere for clarity.

$[\{Tl(S\text{-}t\text{-}Bu)\}_8]$ 2.818(7) Å}.[6a,9a,12] Of the Tl−S distances between monomeric units, one {Tl−S1′ 3.074(2) Å} is a common molecular Tl−S distance while the other {Tl−S2′ 3.346(2) Å} is much longer implying a weaker bonding interaction. The non-bonding S···S distances on the perimeter of the rectangular plane are 3.360(3) Å (2×) and 3.669(3) Å (2×). The shorter distance is a consequence of the ligand's bite angle and the longer distance is slightly smaller than the sum of the van-der-Waals-radii (2 × 1.85 Å).[25] The short Tl···Tl′ distance of 3.5116(4) Å within a dimeric unit is probably caused by the ligand environment and need not indicate a bonding interaction between the metal atoms. Interestingly, this distance is only 0.1 Å longer than in the metal {3.408(6) Å}.[25]

Examination of three distortions from a regular octahedron assists in describing the geometry of the Tl_2S_4 cage of $\mathbf{1}^{2-}$. A tetragonal compression of the Tl···Tl′ vector associated with the relatively fixed Tl−S distances of ca. 3 Å and ligand S1−Tl−S2 angle of 71.76(5)° (Tl···Tl′ 3.5116(4) Å; trans S···S 4.808(3) and 5.138(3) Å). This compression results in a decrease of the Tl−S−Tl′ angles from the ideal value of 90° to ca. 70° and an increase in the dihedral angle between the Tl−S1−S2 and Tl′−S1−S2 planes from the ideal value of 70.5° to ca. 93°. The second distortion might result from crystal lattice effects such that the Tl···Tl′ vector is not orthogonal to the S_4 plane but rather forms an angle of ca. 80°. Lastly, there is a rhombic distortion of the S_4 plane, describable as an elongation of the S2···S2′ vector and a compression of the S1−S2−S1′ angle from the idealized value of 90° to ca. 86°.

Figure 3 contains a packing diagram of the unit cell for $[NEt_4]_2\mathbf{1}$. In the crystal lattice, approximately linear chains of thallium atoms exist with near colinearity of the Tl···Tl′ vectors of $\mathbf{1}^{2-}$ to the *a*-axis. These thallium chains possess a slight zigzag character as evinced by the ca. 3.0° angle between the Tl···Tl′ vector within a dimeric unit and the *a*-axis. The individual dimers are separated by a Tl···Tl distance of 3.937(1) Å. Perpendicular to the thallium chains are nearly coplanar (±0.7 Å) S_4C_{12} fragments creating a "pipeline-like structure" of $1,2\text{-}S_2C_6H_4$-ligands constructed along the *a*-axis. Alternating with the $1,2\text{-}S_2C_6H_4$ layers are layers of cations filling the voids (Figure 3). A closely analogous crystal structure[6b] is observed for $[Tl\{1,1\text{-}S_2CN(i\text{-}Pr)_2\}]_2$, the crystal lattice contains chains of thallium atoms (Tl···Tl within a dimeric unit, 3.58 Å; Tl···Tl between dimeric units, 3.64 Å) aligned parallel to the *c*-axis in a zigzag manner. The zigzag character is dramatically increased compared to $[NEt_4]_2\mathbf{1}$ as can be seen by the ca. 30° angle between the Tl···Tl vectors within a dimeric unit and the *c*-axis.

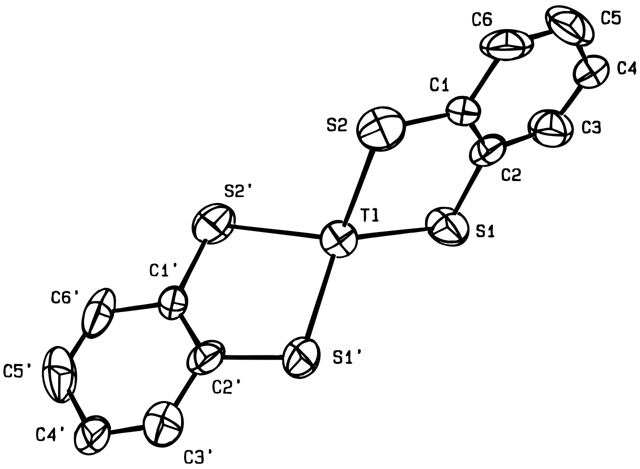

Figure 4. ORTEP plot and numbering scheme of the complex anion of $[NEt_4][Tl(1,2\text{-}S_2C_6H_4)_2]$ with 50% probability ellipsoids.

Recrystallization of $[NEt_4]\mathbf{2}$ from boiling acetone provides yellow crystals suitable for X-ray crystallography. Figure 4 shows the molecular structure of the anion $\mathbf{2}^-$ along with the numbering scheme. The thallium(III) center is situated on a crystallographic 2-fold axis that does not pass through the $1,2\text{-}S_2C_6H_4$-ligands. Expectantly, the Tl(III)−S bond distances of 2.469(4) Å (4×) is significantly shorter than those in $\mathbf{1}^{2-}$ and is to our knowledge the shortest distance so far reported in the literature; for example, Tl−S distances range from 2.563(4) Å in[16] $[N\text{-}n\text{-}Bu_4]_2[Tl\{S_2C_2(CN)_2\}_2Br]$ to 2.613(10) Å in[15a] $[Tl(S_2CNMe_2)_3]$ to 2.870(2) Å in[2b] $[Me_2Tl(pyridine\text{-}2\text{-}thiolato)]$. The shortness in the Tl−S distance is probably a consequence of the +3 formal oxidation state and low coordination number for the thallium center in $\mathbf{2}^-$. The TlS_4 core is distorted from T_d featuring three sets of S−Tl−S angles: (1) S1−Tl−S2 and S1′−Tl−S2′, 89.6(1)°; (2) S1′−Tl−S2 and S1−Tl−S2′, 123.7(1)°; and (3) S1−Tl−S1′, 117.5(1)°, and S2−Tl−S2′, 116.1(1)°. The small angles are due to the ligand's bite angle {89.6(1)°} so that their counterparts become large {123.7(1) and 116.8(average)°}. Similar features have been observed[26] for other $[M(S_2C_6H_3R)_2]^{n-}$ complexes. The distortion from ideal T_d symmetry can be described as an elongation of the molecule. Slight deviations from idealized C_{2v} molecular symmetry are probably due to lattice effects and weak interactions with the cation.

Solution Structure of $[NR_4][Tl(1,2\text{-}S_2C_6H_4)_2]$, Where R = Et and *n*-Bu. In light of the approximately C_{2v} molecular

---

(25) Pauling, L. *The Nature of the Chemical Bond*, 3rd ed.; Cornell University Press: Ithaca, New York 1960.

(26) (a) Bustos, L.; Khan, M. A.; Tuck, D. G. *Can. J. Chem.* **1983**, *61*, 1146. (b) Pfeiffer, J.; Noltemeyer, M.; Meller, A. *Z. Anorg. Allg. Chem.* **1989**, *572*, 145. (c) Greiwe, K.; Krebs, B.; Henkel, G. *Inorg. Chem.* **1989**, *28*, 3713.

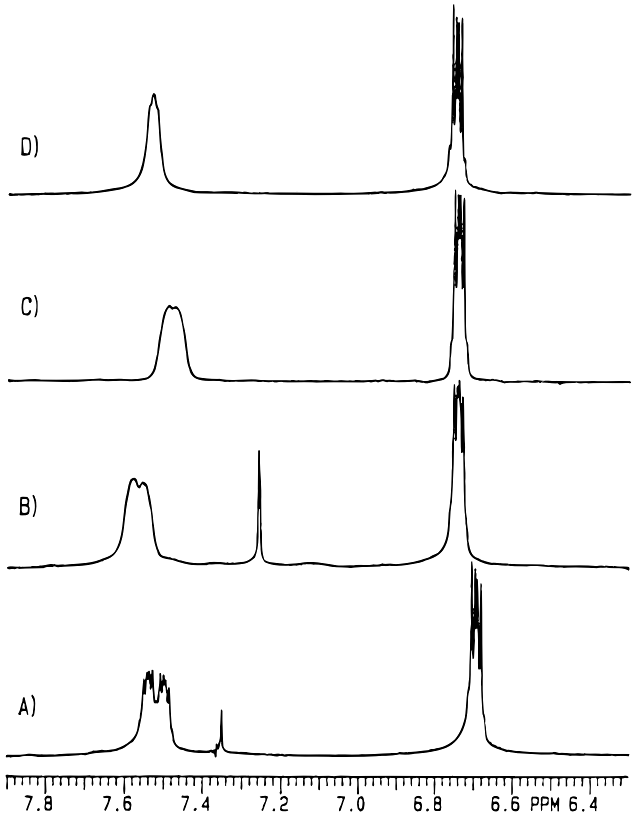

Figure 5. Aromatic region of the ^{1}H NMR spectra of [N-*n*-Bu_4]-[Tl(1,2-$S_2C_6H_4$)$_2$]: (A) acetone-d_6; (B) dimethyl-d_6 sulfoxide; (C) chloroform-*d*; (D) acetonitrile-d_3.

symmetry in the solid state structure, the complexity of the NMR spectra of **2**$^-$ is unexpected. The ^{1}H NMR spectra of [N-*n*-Bu_4]**2** (acetone-d_6, chloroform-*d*, and dimethyl-d_6 sulfoxide) contain two closely spaced low-field multiplets at ca. 7.6-7.4 ppm and a multiplet at ca. 6.7 ppm in the ratio of 1:1:2, respectively. When the solvent is changed to acetonitrile-d_3, the ca. 6.7 ppm multiplet shifts slightly while the two low-field multiplets centered about 7.5 ppm broaden into one resonance at ca. 7.53 ppm. For comparison the aromatic regions of the ^{1}H NMR spectra of [N-*n*-Bu_4]**2** in the four solvents are collected in Figure 5. As with the ^{1}H spectrum, the ^{13}C NMR spectrum (acetone-d_6) contains more peaks than expected: 142.0 (two closely spaced resonances), 134.8, 128.3, 123.0, and 122.5 ppm. Chemical shift assignments were made with the aid of selective decoupling experiments: 142.0 ppm, carbon atom bonded to sulfur; 134.8 and 128.3, d dd (d, $^{1}J_{C-H} = 159$ Hz and dd, $^{2}J_{C-H} = 22$ Hz), meta carbon; and 123.0 and 122.5 ppm, dd (d, $^{1}J_{C-H} = 159$ Hz and d, $^{2}J_{C-H} = 8.6$ Hz), ortho carbon. In acetonitrile-d_3 the ^{13}C NMR spectra contain broadened low intensity signals at 133 and 130 ppm, correlating with the observation of a broadened feature at 7.53 ppm in the ^{1}H NMR spectrum.

A COSY experiment (acetone-d_6) on [N-*n*-Bu_4]**2** confirms the existence of independent coupling between the low-field resonances and the multiplet at ca. 6.7. In addition, the multiplet at ca. 7.6−7.5 ppm is not coupled to the multiplet at ca. 7.5−7.4 (Figure 6). These data indicate that the structure of **2**$^-$ in solution contains two chemically and magnetically inequivalent 1,2-$S_2C_6H_4$ ligands. Further support for this interpretation is obtained from the results of selective decoupling experiments. Irradiation of a low intensity decoupler pulse into the high-field signal led to collapse of the low-field multiplets into two singlets. Attempts to selectively irradiate only one of the two low-field signals gave no clearly interpretable result due to the lack of resolution.

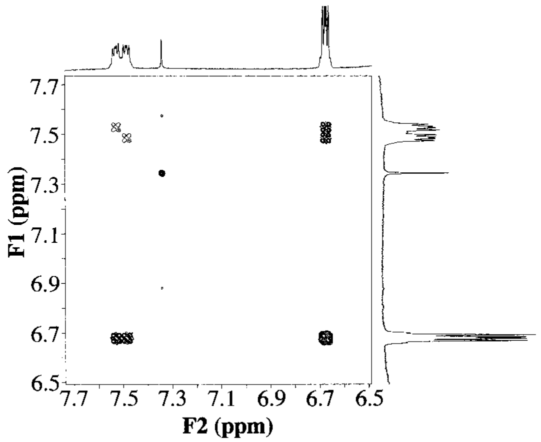

Figure 6. COSY spectrum for the aromatic region of [N-*n*-Bu_4][Tl-(1,2-$S_2C_6H_4$)$_2$] obtained in acetone-d_6.

Vapor pressure osmometry on acetone solutions of [NEt_4]**2** indicate a solution molecular weight of ca. 625 consistent with the formula weight of the anion and cation. This observation is interpreted as suggesting ion pairing between [NEt_4]$^+$ and **2**$^-$ occurs in solution. Tight ion pairing has been identified between tetraalkyl ammonium cations and metallates possessing lone pairs of electrons.[27] The existence of ion pairing clarifies the NMR spectroscopic data. Interaction between the anion and cation in solution reduces the molecular point group of **2**$^-$ from the anticipated C_{2v}, thereby rendering the two $S_2C_6H_4$ ligands inequivalent. As expected the level of ion pairing interaction is weakest in acetonitrile, which has the highest E_T value[28] of the solvents studied, and is stronger in polar aprotic solvents and solvents of low E_T values. In addition the degree of interaction between [NR_4]$^+$ and **2**$^-$ is stronger for the less hindered [NEt_4] salt, which suggests the phenomenon is not an intramolecular process solely involving the anion. In acetonitrile-d_3 (21 °C) the ^{1}H NMR spectrum of [NEt_4]**2** contains two closely spaced low-field multiplets at ca. 7.6−7.4 ppm and a multiplet at ca. 6.7 ppm in the ratio of 1:1:2, respectively, which resembles the spectrum of [N-*n*-Bu_4]**2** in dimethyl-d_6 sulfoxide. Cooling the [NEt_4]**2** sample to ca. −40 °C provides a frozen spectrum, which resembles the spectrum of [N-*n*-Bu_4]**2** in acetone-d_6, containing two closely spaced low-field multiplets at ca. 7.55 and 7.47 ppm and a multiplet at ca. 6.74 ppm in the ratio of 1:1:2, respectively. In contrast the cold temperature spectrum of [N-*n*-Bu_4]**2** (acetonitrile-d_3, ca. −40 °C) provided an intermediate exchange spectrum close to the coalescence region. Complete variable temperature NMR spectroscopic studies are inconclusive due to decomposition of the samples at the higher temperature near the fast exchange limit. In summary, the collection of observations is consistent with the existence of an equilibrium between the tight ion-pair [NR_4]**2** and the free ions.[29]

---

(27) (a) Bertini, I.; Luchinat, C.; Borghi, E. *Inorg. Chem.* **1981**, *20*, 306. (b) Chen, N; Witton, P. J.; Holloway, C. E.; Walker, I. M. *J. Coord. Chem.* **1988**, *19*, 113. (c) Drago, R. S. *Physical Methods for Chemists*, 2nd ed.; Saunders College Publishing: Ft. Worth, TX, 1992; chapter 8.

(28) Reichardt, C. *Angew. Chem., Int. Ed. Engl.* **1965**, *4*, 29.

(29) (a) Dehmlow, E. V.; Dehmlow, S. S. *Phase Transfer Catalysis*; VCH Verlagsgesellschaft: Weinheim, Germany 1983. (b) Starks, C. M.; Liotta, C. L.; Halpern, M. *Phase-Transfer Catalysis: Fundamentals, Applications, and Industrial Perspectives*, Chapman & Hall: New York, 1994.

Concluding Remarks

Reaction of thallium salts and 1,2-$(NaS)_2C_6H_4$ in a 1:2 stoichiometry affords reliable routes to either the thallium(I) product $[NEt_4]_2[\{Tl(1,2\text{-}(\mu\text{-}S)_2C_6H_4)\}_2]$ ($[NEt_4]_2$**1**), under anaerobic conditions, or to the thallium(III) product $[NEt_4][Tl(1,2\text{-}S_2C_6H_4)_2]$ ($[NEt_4]$**2**), under aerobic conditions. However, the thallium(I) complex does not appear to be an intermediate in the preparation of the thallium(III) complex because exposing anaerobically prepared solutions to air does not produce the thallium(III) product. Instead, a series of color changes occur, eventually leading to an intractable black solution. This observation is in contrast to the behavior of other low valent p-block complexes. For example, treating $[Sn(1,2\text{-}S_2C_6H_4)_2]^{2-}$ or $[Sb(1,2\text{-}S_2C_6H_4)_2]^{-}$ with air affords excellent conversion to the high valent product, $[Sn(1,2\text{-}S_2C_6H_4)_3]^{2-}$ or $[Sb(1,2\text{-}S_2C_6H_4)_3]^{-}$, respectively.[23,30]

An additional feature of $[NEt_4]_2$**1** is the presence of a nearly linear chain of thallium atoms in the crystal lattice, which aligns along the *a*-axis, and coplanarity of the $S_2C_6H_4$ fragments with the bc-plane. Noteworthy, this alignment along the *a*-axis appears to be unsupported by bridging interactions since the shortest Tl···S interaction between dimeric units is >5.8 Å. Conceivably, Tl···Tl interactions between dimeric units may be responsible for attainment of the nearly linear chains of thallium atoms in the crystal lattice. In contrast, while some of the $[\{Tl(1,1\text{-dithiolene})\}_2]$ complexes possess analogous Tl_2S_4 dimers, the Tl···Tl vectors are offset by at least 30° with respect to a crystallographic axis and the Tl···S interactions between dimeric units are within 10% of the Tl−S bond lengths within a dimeric unit.[6] In light of the slow continuous color changes that occur as $[NEt_4]_2$**1** is air oxidized and the tendency for the class of complexes to exhibit Tl···Tl interactions between dimeric units, we are continuing our investigations into the oxidation chemistry of these classes of thallium(I) complexes.

Acknowledgment. We are grateful to Dr. Jon Kirchhoff for time and advise involving electrochemistry and to Dr. Bruce Cheeseman for assistance on NMR spectroscopy. We are also indebted to the State of Ohio Academic Challenge Program for the funds for a high-field NMR spectrometer and for support of this research and to the College of Arts and Sciences for support of the X-ray crystallographic facilities. Acknowledgment is made to the donors of the Petroleum Research Fund, administered by the American Chemical Society, for support of this research.

Supporting Information Available: Text giving experimental details and a full listing of crystallographic data for $[NEt_4]_2$**1** and $[NEt_4]$**2** including tables of crystal data and structure refinement, positional parameters, general displacement parameters, bond distances and bond angles (8 pages). See any current masthead page for ordering information and Internet access instructions.

IC951411X

---

(30) Föcker, A.; Kirschbaum, K.; Uhlenbrock, S.; Klein, R.; Krebs, B.; Giolando, D. M. Unpublished results.